We are IntechOpen,
the world's leading publisher of
Open Access books
Built by scientists, for scientists

6,900
Open access books available

185,000
International authors and editors

200M
Downloads

154
Countries delivered to

Our authors are among the

TOP 1%
most cited scientists

12.2%
Contributors from top 500 universities

CLARIVATE ANALYTICS
BOOK CITATION INDEX
INDEXED

WEB OF SCIENCE™

Selection of our books indexed in the Book Citation Index
in Web of Science™ Core Collection (BKCI)

Interested in publishing with us?
Contact book.department@intechopen.com

Numbers displayed above are based on latest data collected.
For more information visit www.intechopen.com

Pancake Bonding Seen through the Eyes of Spectroscopy

Alexis Antoinette Ann Delgado, Alan Humason and Elfi Kraka

Abstract

From local mode stretching force constants and topological electron density analysis, computed at either the UM06/6-311G(d,p), UM06/SDD, or UM05-2X/6–31++G(d,p) level of theory, we elucidate on the nature/strength of the parallel π-stacking interactions (i.e. pancake bonding) of the 1,2-dithia-3,5-diazolyl dimer, 1,2-diselena-3,5-diazolyl dimer, 1,2-tellura-3,5-diazolyl dimer, phenalenyl dimer, 2,5,8-tri-methylphenalenyl dimer, and the 2,5,8-tri-t-butylphenalenyl dimer. We use local mode stretching force constants to derive an aromaticity delocalization index (AI) for the phenalenyl-based dimers and their monomers as to determine the effect of substitution and dimerization on aromaticity, as well as determining what bond property governs alterations in aromaticity. Our results reveal the strength of the C⋯C contacts and of the rings of the di-chalcodiazoyl dimers investigated decrease in parallel with decreasing chalcogen⋯chalcogen bond strength. Energy density values H_b suggest the S⋯S and Se⋯Se pancake bonds of 1,2-dithia-3,5-diazolyl dimer and the 1,2-diselena-3,5-diazolyl dimer are covalent in nature. We observe the pancake bonds, of all phenalenyl-based dimers investigated, to be electrostatic in nature. In contrast to their monomer counterparts, phenalenyl-based dimers increase in aromaticity primarily due to CC bond strengthening. For phenalenyl-based dimers we observed that the addition of bulky substituents steadily decreased the system aromaticity predominately due to CC bond weakening.

Keywords: local stretching force constant, dimerization, pancake bonding, aromaticity, 2e/mc bonding

1. Introduction

The initial concept of "pancake bonding" was constructed by Mulliken and Person as to characterize the overall shape and bonding mechanisms of donor-acceptor π systems [1]. More recently the term "pancake bonding" has primarily been used to describe the formation of stabilizing parallel π–π interactions between two or more open-shell free radicals, those of which are typically planar and/or consist of light-atoms [2–4]. Such interactions have received a considerable amount of interest as they allow one to synthesize novel radical-based materials, via electron or hole through-space delocalization, that exhibit unique magnetic [5], optical [6], and electronic properties (i.e. conductive polymers, organic conductors) [7].

Generally, free radical species are short lived and exist in low concentration as two radicals will typically react to form a single covalently bonded dimer, or σ-dimer. However, when radicals are sterically hindered against approaching within a covalent bonding distance, they can exist as a stable, spin-paired, open shell species. Unlike general non-covalent interactions between closed-shell species (i.e. van der Waals), the open-shell radicals have been said to undergo stabilization with each other via through-space π-stacking 2e/mc distributed interactions (i.e. pancake bonding). This 2e/mc bonding (i.e. pancake bonding) is a result of overlapping antibonding (π^*) singly occupied molecular orbitals (SOMO) of the two monomer radicals with highly delocalized π-electrons [8]. It is noted that magnetic experimental analysis has found the spin pairing of pancake bonded dimers to be diamagnetic with an overall spin density of zero (i.e. singlet electronic state) [9]. The overlapping of antibonding (π^*) SOMOs is the basis of pancake bonds as this interaction leads to the following distinctive features [4]: i) contact bond distances that are beyond the usual $C(sp^3)$–$C(sp^3)$ bond length (1.54 Å) but are also much shorter than the bonds of closed shell dimers that are held together by vdW forces (sum of vdW radii = 3.40 Å) (ii) due to direct atom-to-atom overlap, SOMO-SOMO overlapping strongly favors configurations that yield maximum overlap orientations which lower the energy of the two radical SOMOs iii) low lying singlet (-singlet-singlet) and triplet (singlet-triplet) electronic excited states, iv) negative singlet-triplet splitting energies (i.e., ΔE_{ST} = E(singlet) – E(triplet)) for stable open shell singlet pancake bonded complexes [10] and v) interaction energies larger than those of vdW interactions. Bond dissociation energies (BDE) of pancake bonded system have been estimated to be smaller than those of a normal covalent system but larger than dimers subject to typical π-stacking where this type of π-stacking is observed for DNA base pairs [11] (vdW π stacking interactions and pancake bonds are different). Several works analyzed the related binding energies (BE), splitted into two contributions, a destabilizing stabilizing vdW part, E_{vdW}, and a stabilizing energy, E_{SOMO}, associated with the bonding overlap of the singly occupied SOMO [12]. E_{SOMO} yields a reasonable description of the SOMO-SOMO overlap contribution to BE and it has been suggested that E_{SOMO} can be estimated from the difference between E(singlet) – E*(triplet), where E*(triplet) is the triplet energy evaluated for the singlet geometry [12].

BE, E_{SOMO} and SOMO-SOMO overlap have been utilized as to further explain the nature of these systems [8, 13]. It was argued that the dimerization of such radicals exhibit covalent bonding character as the spin-pairing of the electrons in the SOMO leads to a filled highest occupied molecular orbital (HOMO) and a corresponding empty antibonding LUMO [14]. In this situation, the interaction occurs at rigid rotational geometries, due to SOMO-SOMO overlapping, which is different from π-stacking in which various rotational orientations are possible [15]. On the other hand, dispersion and/or van der Waals interactions have been suggested to play important roles in the overall stabilization of these dimers [14]. Thus, the nature of pancake bonds between 1,2-chalcogen-3,5-diazol radicals and phenalenyl-based radicals remains in debate to the present day.

A CSD database survey based upon 35 cis-cofacial dimers composed of HCNSSN radicals, with C–C contact distances ranging between 2.75 to 3.50 Å, showed that S⋯S contact bond distances ranged from 2.93 to 3.30 Å [8]. These S⋯S contact bond are much shorter than the vdW distance between two sulfur atoms (4.06 Å) [16], in the case of two spherical sulfur atoms the vdW distance has been computed to be 3.60 Å. A CSD database survey based on 12 cis-cofacial 1,2-diselena-3,5-diazolyl dimers, with C⋯C contact distances between 2.80 and 3.50 Å, found the average Se⋯Se contact distance to be 3.26 (s = 0.05) [8]. This average Se⋯Se contact distance is slightly smaller than the vdW distance between spherical Se

atoms (3.32 Å). Previously computed dissociation energies have suggested that dimers of R-CNSeSeN radicals dimers are more binding than dimers of R-CNSSN radicals; relative binding energy values were also observed to be analogous to vdW interactions [8].

1,2-chalcogen-3,5-diazole dimers: Within the past two decades di-chalcogen-diazole radicals, such as 1,2-dithia-3,5-diazolyl (i.e. HCNSSN) and 1,2-diselena-3,5-diazolyl (i.e. HCNSeSeN) radicals, and their derivatives have been a subject of many investigations [17]. The rings of HCNSSN and HCNSeSeN are rich in π-electrons and have π^* singly occupied molecular orbitals (SOMO). The 1,2-dithia-3,5-diazolyl and 1,2-diselena-3,5-diazolyl radicals have been experimentally observed to result in stable dimerizations in the solid state where, in most cases, the neutral radicals prefer to be oriented with their faces parallel to one another (cis-cofacial) in order to achieve a configuration that supports maximum π^*-π^* (SOMO-SOMO) overlapping observed as two electron/eight-center (2e/8c) π-stacking (i.e. pancake bonding) interactions. A notable feature of HCNSSN and HCNSeSeN dimers are their four long chalcogen-chalcogen bonds (i.e. contacts) ranging between 2.2 and 4.0 Å. HCNSSN and HCNSeSeN dimers have been suggested to stabilize via a combination of π and σ aromaticity [13].

Phenalenyl-based dimers: In solution, phenalenyl radicals maintain chemical equilibrium via the formation of a σ-bonded dimer [18]. Due to the very high symmetry of the radical phenalenyl monomer, a unpaired electron is delocalized across all α-positions of the phenalenyl framework excluding the central carbon atom of the monomers [19]. As noted in the work of Kubo [19], the thermodynamic stability of such carbon-centered radical species increases as the delocalization of unpaired electrons across a system increases [19]. Another interesting feature of phenalenyl dimers and their derivatives (i.e. carbon-centered hydrocarbon radicals) is due to the formation of unique two-electron/twelve-center (2e/12c) π-stacking interactions between these spin-delocalized hydrocarbon radicals [20] as verified by NMR [21]. The hexagonal arrangement of the SOMO of the phenalenyl radicals enables perfect π-π overlap in both eclipsed and staggered stacking configurations, the staggered stacking configuration is favored over the eclipsed configuration due to shorter π-π contacts as a result of less atom-atom repulsion [19]. It is mentioned, that various phenalenyl derivatives, which demonstrate π-π stacking (i.e. pancake bonding), have been experimentally identified via single crystal X-ray diffraction (XRD) [22]. The formation of σ-bonded phenalenyl radical dimer can be inhibited by substituting the carbon atoms of the phenalenyl rings, at the 2,5,8-positions, with *tert*-butyl groups as a π-bonded dimer results from the sterically hindered phenalenyl radicals [19]. Moreover, X-ray studies have revealed that the application of sterically hindered substituents (i.e. *tert*-butyl groups) on phenalenyl radicals prevent σ-dimerization and results in a π-bonded dimer with a face-to-face stacking distance, twice that of the σ-bonded dimer, at a length of of 3.2 Å [23]. This π-π contact (face-to-face) stacking distance is characteristic to pancake bonding as this length is shorter than that of a vdW complex and is beyond the length of a coventional covalent bond. Bond dissociation energy (BDE) for systems containing carbon radicals such as phenalenyl have been estimated to be around 10 kcal/mol [11]. Because σ-bonded and π-bonded phenalenyl-based dimers are close in energy the existence of the pancake bonded dimer as a fluxional molecule has been reviewed [12].

Although many experimental and computational have been conducted for the dimerizations of 1,2-chalcogen-3,5-diazol and phenalenyl-based radicals, the intrinsic strength of these interactions remains unclear. While popular BDE and its decomposition [24] provides valuable information about the stabilizing forces involved in bond formation (in the case of pancake bond in particular in the

formation of 2e/mc interactions), BDE does not adequately describe the intrinsic strength of a bond [25–27]. Because BDE measures the overall effect of bond breakage it contains the electronic reorganization and geometrical relaxation of the fragments upon dissociation. Therefore, we introduced in this work an intrinsic bond strength measure based on vibrational spectroscopy. Unlike BDE, the local stretching force constant (k^a), derived from local vibrational modes [25], conserves the geometry and electronic structure of all bonds/interactions. k^a provides a direct description of intrinsic bond strength and has been applied successfully applied to assess the intrinsic bond strengths for a variety of covalent interactions including ultra long C–C bonds, carbon-halogen bonds and non-covalent interactions such as hydrogen, tetrel, pnicogen, chalcogen and halogen bonds; see Ref. [25] and citations therein.

In this study, we applied the local mode analysis [25] complemented with the RING puckering analysis of Cremer and Pople [28] and Bader's quantum theory of atoms in molecules (QTAIM) analysis of the electron density [29] to quantify the strength of the pancake bonds in six spin-paired, open-shell singlet state dimers **1–6** (shown in **Figure 1**) and and to learn more about their nature. Species **1–3** are 1,2-chalcogen-3,5-diazole dimers which contain sulfur (**1**), selenium (**2**), and tellurium atoms (**3**); it is noted that **3** is a prototypal (i.e. theoretical) species. Species **4–6** are phenalenyl-based dimers in which the bulkiness of substituents increase as follows: phenalenyl dimer (**4**) < 2,5,8-trimethylphenalenyl dimer (**5**) < 2,5,8–*tert*-butylphenalenyl (**6**). The aromatic character of the dimer species (**4–6**) was also explored, in particular the role of the aromaticity for the stabilization of phenalenyl-based dimers. In summary, special focus was on: i) to assess the intrinsic bond strengths of the 2e/mc interactions for selected species, ii) to quantify the ring strengths of the selected species, iii) to determine if the pancake bonds of these species are covalent in nature, iv) to elucidate on the effect of substituents on the aromaticity of phenalenyl-based species, v) to determine, for phenalenyl-based dimers, the effect of dimerization on the aromaticity for phenalenyl-based species,
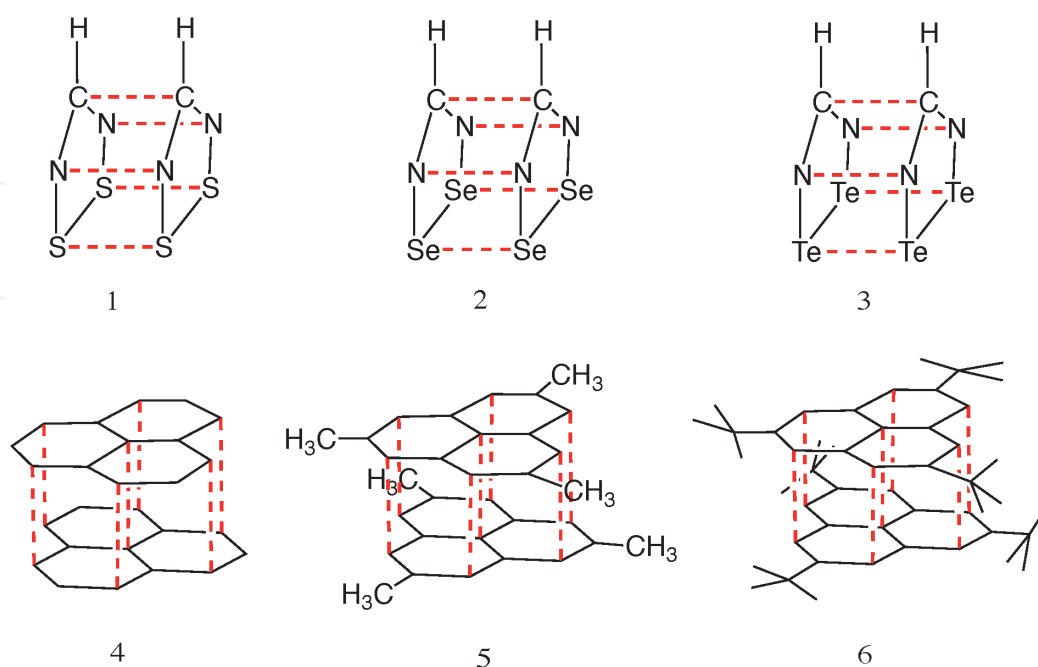

Figure 1.
Species investigated in this work. 1) 1,2-dithia-3,5-diazolyl (HCNSSN) dimer 2) 1,2-diselena-3,5-diazolyl (HCNSeSeN) dimer 3) 1,2-tellura-3,5-diazolyl (HCNTeTeN) dimer 4) phenalenyl dimer. 5) 2,5,8-tri-methylphenalenyl dimer. 6) 2,5,8-tri-t-butylphenalenyl dimer. Detected pancake bonds (2e/mc) (i.e. targeted contact bonds and interdimer CC bonds) are denoted in red.

and vi) to determine what bond property, of the phenalenyl-based species investigated, predominately governs changes in aromaticity.

2. Computational methods

Local mode theory: Since the underlying theory behind the derivation of local vibrational modes is elaborated on in Ref. [25] the following text briefly covers the fundamental aspects. Every vibrational mode, being associated with potential and kinetic energy contributions, is subject to two mode-to-mode coupling mechanisms, electronic coupling and kinematic (mass) coupling [30]. As a result the normal modes remain perpetually delocalized over a molecule and cannot be directly used to assess chemical bond strength [25]. Solution of the vibrational secular equation (i.e. the Wilson equation) eliminates the electronic coupling as a result of force constant matrix diagonalization. The kinematic coupling which remains is eliminated in the local mode theory via a modified version of the Wilson equation that uses mass-decoupled Euler–Lagrange Equations [25]. This leads to local vibrational modes, associated with local mode frequencies ω^a and local mode force constants k^a that can serve as a quantitative bond strength measure [25] which we applied to assess the strength all 2e/mc interactions (i.e. pancake bonds) of species **1**–**6** (see **Figure 1**). Stretching force constants k^a can be transformed into relative bond strength orders (BSO) n which are more convenient for comparison, via a generalized Badger rule [31], leading to the following power relationship between these two quantities: BSO $n = A \ (k^a)^B$. Constants A and B can be determined from two reference molecules with known k^a and BSO n values and the requirement that for a zero k^a value the BSO n is also zero.

In our study we used the CC single bond of ethane with BSO $n = 1$ and the CC double bond of ethene with BSO $n = 2$ as references [32]. In addition to BSO n values for the C···C contacts, BSO n values for N···N, S···S, Se···Se, and Te···Te bonds of the dichalcodiazolyl species **1**–**3** were derived using the same power relationship. For dimers **4**–**6**, aside from deriving the BSO n values for the central C–C bonds, we also computed the BSO n values for the outer C···C contacts which are established between six carbon atoms of each monomer (see **Figure 1**).

Aromaticity index based on local modes: π delocalization in species **4**–**6** was determined via an aromatic delocalization index (AI) derived from local force constants following the procedure of Kraka, Cremer and co-workers [33, 34]. In contrast to the HOMA index [35] which is based upon optimal bond lengths, which sometimes tend to fail for this purpose [33], the AI is based on local stretching force constants and bond strength orders (BSO n). As a reference, we used benzene with an AI value of 1.00 and assigned BSO n value of 1.451 [33].

BDEs for **1**–**6** were derived via potential energy curves by varying the interdimer distance from 2.5 to 8.0 Å, using increments of 0.1 Å around and 1.0 Å further away from the equilibrium geometry, followed by a constrained optimization. By calculating BDEs via potential energy curves any basis set superposition errors can be avoided, such errors have been reported to as large as 16 kcal/mol in these complexes when the BDE is calculated from the differences between dimer and monomer energies [14]. The covalent character of the pancake bonds was assessed with the Cremer-Kraka criterion [36, 37] of covalent bonding within the framework of Bader's QTAIM [29]. The Cremer-Kraka criterion is composed of two conditions; (i) existence of a bond path and bond critical point $r_b = b$ between the two atoms under consideration; (ii) sufficient condition: the energy density $H(r_b) = H_b$ is smaller than zero. $H(r)$ is defined as $H(r) = G(r) + V(r)$, where $G(r)$ is the kinetic

energy density and $V(r)$ is the potential energy density. A negative $V(r)$ corresponds to a stabilizing accumulation of density whereas the positive $G(r)$ corresponds to depletion of electron density [36]. As a result, the sign of H_b indicates which term is dominant [37]. If $H_b < 0$, the interaction is considered covalent in nature, whereas $H_b > 0$ is indicative of electrostatic interactions.

Model chemistry used: To describe the spin-paired open shell singlet states, we applied a single determinant broken-symmetry (BS) unrestricted ansatz, which works well for systems with small singlet-triplet gaps [38, 39], combined with a density functional theory (DFT) approach. We refrained from a multi-reference description, such as CASSCF, which has been mostly applied to unsubstituted species **4** with a relatively small active space and basis sets [40]. We also refrained from post-SCF methods, such as Møller-Plesset perturbation theory of second order, which has shown to over-bind in the case of dimer complexes with pancake bonds and may results in an unrealistic C⋯C contact distance of 2.8 Å [14].

A reliable description of pancake bonding requires a careful choice of DFT functional. The popular B3LYP functional [41, 42] does not describe dispersion well whereas the dispersion corrected ωB97X-D [43] functional sometimes leads to inconsistent results [44]. It was reported that the M06-2X functional [45] yields generally shorter C⋯C contact distances [46] whereas the C⋯C contact distances based off the M05-2X functional [47] agree well for complexes for **4–6** with experimental values [48]. On the other hand, the M06 functional has shown to be well parameterized for describing chalcogens (i.e. sulfur, selenium and tellurium atoms) [45]. Another important part of the model chemistry is the basis set. We tested both, Pople's augmented 6–31++G(d,p) double zeta [49, 50] and 6-311G(d,p) triple zeta basis sets [51]. For the Te atom we applied the SDD basis set [52] which uses the Stuttgart-Dresden pseudopotentials [53] to account for relativistic effects. Guided by our test calculations, we decided to use for our study the BS-UM06/6-311G(d,p) model chemistry for **1–2**, BS-UM06/SDD for **3**, and BS-UM05-2X/6–31++G(d,p) for **4–6**.

Software used: All DFT geometry optimizations and frequency calculations were carried out using the Gaussian program package [54]. The following local mode analysis and the aromaticity delocalization index (AI) study was carried out with the LModeA software [55]. The QTAIM analysis was performed with the AIMALL program [56] For the rings of the di-chalcodiazoyl dimers (**1–3**), which do not contain a central atom, we used the ring puckering program [57] followed by LMA, as to obtain the local mode properties of the rings.

3. Results and discussion

It is noted that in regard to the text which follows, the terms contact bonds, π-π stacking interactions, and face-to-face interactions loosely refer to pancake bonds while interdimer/central C-C bonds refer to the C-C bond established in the center of two monomers. **Table 1** summarizes the calculated bond distances (R_{calc}), experimental bond distances (R_{exp}), calculated bond dissociation energies (BDE_{calc}), experimental bond dissociation energies (BDE_{exp}), local stretching force constants (k^a), local mode vibrational frequencies (ω^a), bond strength orders (BSO n), electron densities (ρ_b), and energy densities (H_b) for the targeted CC bonds of of targeted contacts bonds of dimers **1–6** and rings of **1–3**. **Table 2** summarizes symmetry, singlet and triplet C⋯C contact distance (R(CC)), energy values of SOMOs (E_{SOMO}), and triplet/singlet (ΔE_{ST}) for all species investigated in this work (**1–6**). **Figure 2** shows the equilibrium geometries for the HCNTeTeN **3** dimer (C_2) in

No.	Species	R_{calc}	R_{exp}	BDE_{calc}	BDE_{exp}	k^a	ω^a	BSO n	ρ_b	H_b
1	HCNSSN									
	Ring	3.071		−5.8	−5.3 [8]	0.657	147	0.214	0.016	0.005
	C–C	3.036	3.18			0.208	243	0.083	0.041	0.007
	N-N	3.034				0.128	176	0.056	0.052	0.004
	S-S	3.125				0.192	143	0.078	0.104	−0.000
2	HCNSeSeN									
	Ring	3.210		−4.7	N/R	0.302	72	0.113	0.015	0.004
	C–C	3.119	3.31			0.080	151	0.038	0.034	0.006
	N-N	3.152				0.074	134	0.036	0.042	0.003
	Se-Se	3.313				0.151	80	0.064	0.098	−0.000
3	HCNTeTeN, C_{2v}									
	Ring	3.514		−6.0	N/A	0.049	23	0.021	0.013	0.001
	C–C	3.219	N/A			0.029	83	0.014	0.036	0.006
	N-N	3.333				0.032	29	0.016	0.039	0.006
	Te-Te	3.840				0.045	123	0.022	0.073	0.002
4	HCNTeTeN, C_2									
	Ring	3.413		−8.4	N/A	0.162	43	0.062	0.018	0.002
	N-N	3.342				0.112	165	0.045	0.046	0.009
	Te-Te	3.820				0.038	65	0.018	0.086	0.003
	N-Te	3.510				0.045	78	0.021	0.069	0.007
5	Phenalenyl									
	Peripheral C–C	3.110	N/A	−11.0	N/A	0.366	123	0.136	0.072	0.005
	Central C–C	3.152	N/A			0.293	288	0.113	0.063	0.006
6	tMP									
	Peripheral C–C	2.997	3.053	−14.8	N/R	0.172	64	0.074	0.090	0.006
	Central C–C	3.093	3.145			0.167	217	0.072	0.070	0.007
7	tTBP									
	Peripheral C–C	3.391	3.306	−12.4	−9.5 [59]	0.194	68	0.081	0.047	0.003
	Central C–C	3.287	3.201			0.147	204	0.065	0.050	0.005

*The UM06/6-311G(d,p) methodology used for **1** and **2**, UM06/SDD for **3**, and UM05-2X/6–31++G(d,p) for **4**, **5** and **6**. N/A, not applicable; N/R, not reported.*

Table 1.
*Summary of calculated bond distances (R_{calc}) in Å, experimental bond distances (R_{exp}) in Å, bond dissociation energies (BDE_{calc}) in kcal/Mol, experimental bond dissociation energies (BDE_{exp}) in kcal/Mol, vibrational spectroscopy data, electron densities (ρ_b) in $e/Å^3$, and energy densities (H_b) in $h/Å^3$ of the targeted contacts bonds and rings of dimers **1–6** (see **Figure 1**).*

singlet and triplet states. **Figure 3** shows the various conformations of the phenalenyl dimer in the triplet state where the red lines indicate detected C⋯C contacts. **Figure 4** show the generated Morse potential curves of dimers **1–6**. **Figure 5** shows the correlation between BSO n values and the local stretching force constants k^a of **1–6**. **Figure 6** showcases the BSO n(CC) values, corresponding CC bond lengths, AI values, bond weakening/strengthening parameters (WS), and bond alteration parameters (ALT) for the carbon ring structures and the outer ring

No.	Species	Dimer	Monomer	Singlet	Triplet	E_{SOMO}	ΔE_{ST}
		Symmetry	Symmetry	R(CC)	R(CC)		
1	HCNSSN	C_{2v}	C_{2v}	3.036	3.452	−15.61	−2.17
2	HCNSeSeN	C_{2v}	C_{2v}	3.119	3.208	−13.90	−2.09
3	HCNTeTeN	C_{2v}	C_{2v}	3.165	3.362	−13.26	0.96
3	HCNTeTeN	C_2	C_2	3.563	3.104	−8.46	−1.35
4	Phenalenyl	D_{3d}	C_{3H}	3.152	3.622	−12.97	−5.98
5	tMP	D_{3d}	C_{3H}	3.093	3.744	−19.26	−5.44
6	tTBP	S_6	C_{3H}	3.281	3.855	−6.11	−3.13

Table 2.
*Symmetry of dimer and monomer, singlet and triplet face-to-face distances (R(CC)) in Å, energy values of SOMOs (E_{SOMO}) in kcal/Mol and triplet/singlet splitting (ΔE_{ST}) in kcal/Mol for comlexes **1–6** (see **Figure 1**) calculated at corresponding levels of theory.*
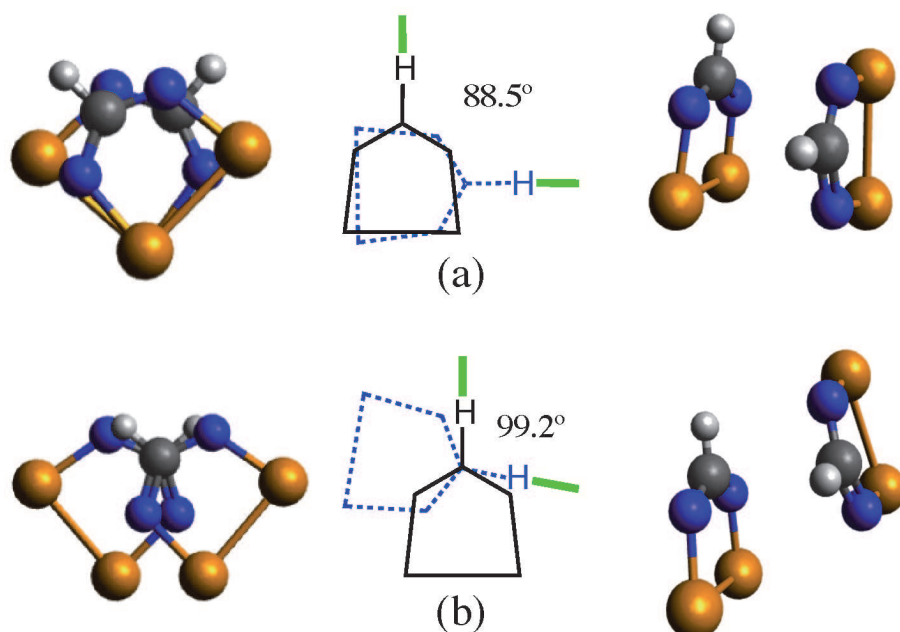
Figure 2.
*Equilibrium geometries for HCNTeTeN (**3**) dimers in C_2 symmetry. a) Singlet. b) Triplet.*

structures of phenalenyl, 2,5,8-trimethylphenalenyl, and 2,5,8-tri-t-butylphenalenyl monomer radicals and dimers.

3.1 Energetics

Identifying pancake bond interactions: As shown in **Table 2**, the E_{SOMO} values for dimers **1–6** range between −6.11 and −19.26 kcal/mol where **5** acquires the largest E_{SOMO} value. We note that the E_{SOMO} value of **6** is in good agreement with the ST-splitting of −6.64 kcal/mol derived from ESR experiments [21]. As shown in **Table 2** the $\Delta E_{(ST)}$ is small and negative for dimers **1–6** with **3** in C_2 symmetry. These results are in line with the notion that the formation of pancake bonded dimers requires the spin-paired singlet state to be energetically favored over the triplet state.

From singlet to the triplet state, the central C–C bond distances in dimers **1** and **2** increase from 3.04 Å and 3.12 Å to 3.45 Å and 3.21 Å, respectively. No alterations in
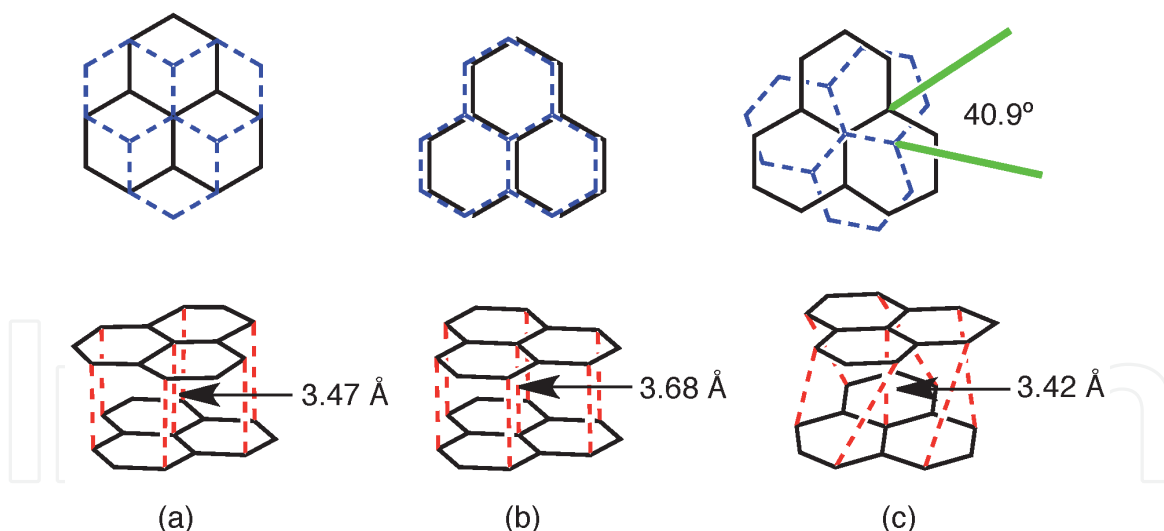
Figure 3.
Conformations of the phenalenyl dimer in the triplet state. a) Staggered. b) Eclipsed. c) Intermediate geometry. The red lines indicate detected π-π contacts. Bond distances for the central CC bond between the two monomers are given.
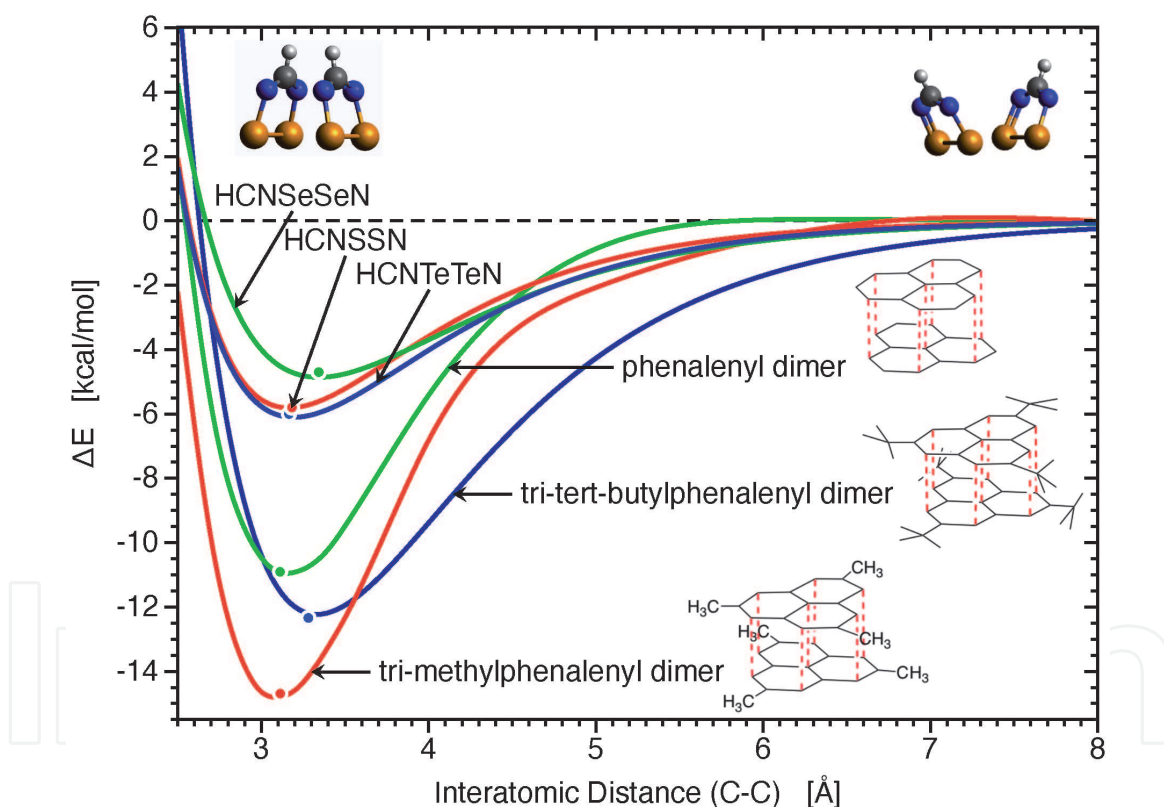

Figure 4.
Dissociation curves for dimers 1 and 2 (UM06/6-311G(d,p), 3 (C$_{2v}$) (UM06/SDD), and 4–6 (UM05-2X/6–31++G(d,p)).

the rotational alignments amongst these two species were observed. Unlike for dimers of **1** and **2**, we observe that, in the singlet state of the HCNTeTeN dimer (**3**) one monomer rotates about the CC central axis by 88.5°, resulting in a C$_{2v}$ symmetry for the dimer. Moreover, the triplet state of the HCNTeTeN dimer (**3**) involves the rotation of a monomer, about the central C-C axis, by 99.2° and results in a C$_2$ symmetry for the dimer (see **Figure 2**).

The ΔE$_{ST}$ values of **1–3**, where **3** is in C$_2$ symmetry, indicate stable arrangements (see **Table 2**). In the case of **3**, which is common in symmetry to dimers **1** and **2** (C$_{2v}$),
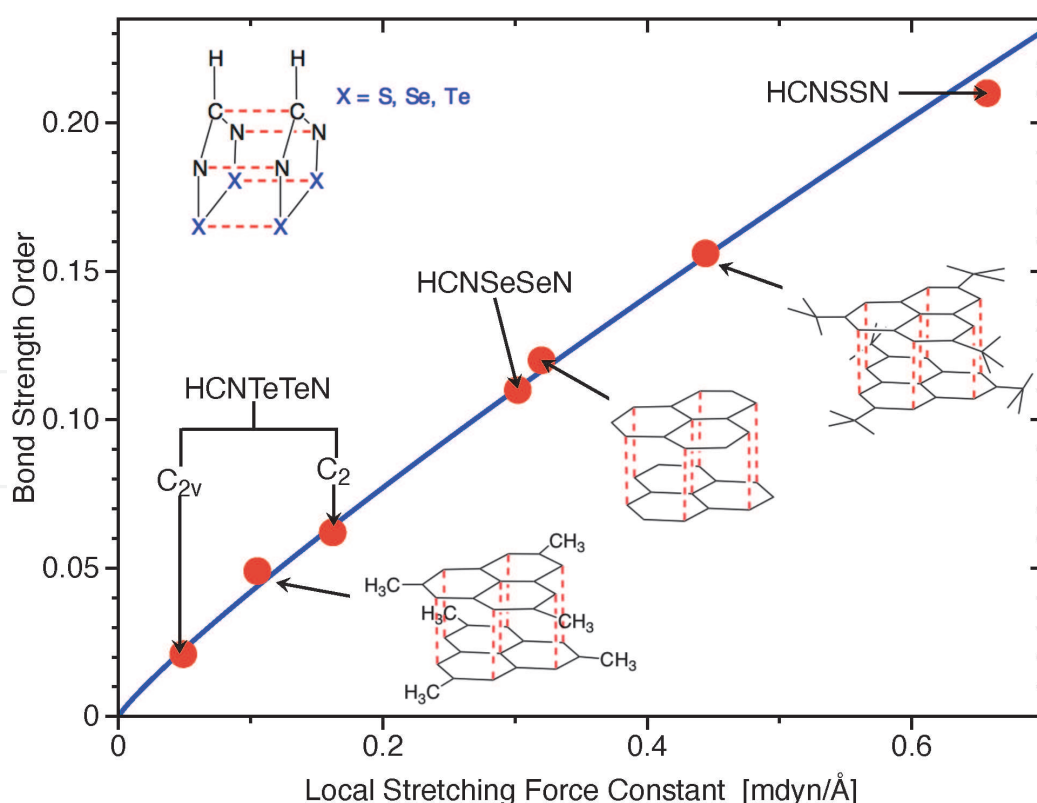
Figure 5.
The relationship between BSO n and force constants of dimers 1–6 calculated with UM06/6-311G(d,p) (1 and 2), UM06/SDD (3), and UM05-2X/6-31++G(d,p) (4–6). BSO n(ring) values for 1–6 were computed via in accordance to the level of theory used.

the triplet state is lower than the singlet state ($\Delta E(_{ST})$ = 0.96 kcal/mol) reflecting an unstable dimer structure as no pancake bonding is formed. We note that for the lower energy structure of **3** (C_2) BCP's were detected for Te···Te, Te···N, and N···N contacts, being consistent with the observations of Gleiter and Haberhauer [58], in which the reorientations of dithiatriazine molecules favored the formation of S···N and S···C interactions over the the formation of a C···C contacts. Notably, unlike the other dichalcodiazoyl dimers, the central C–C distance of the **3** (C_2) dimer, from the singlet to the triplet state, decreases from 3.56 Å to 3.10 Å. Going from a C_{2v} symmetry to C_2 symmetry the E_{SOMO} value of **3** changes from −13.26 kcal/mol to −8.46 kcal/mol. These results indicate that there are attractive interactions between the monomers of **3** (C_2) that are unrelated to SOMO-SOMO overlap. Overall, the results based on **3** in C_{2v} and symmetry C_2, suggest that chalcogen···chalcogen bonds and the electrostatic attraction between a chalcogen and a less electronegative atom play significant roles in the stabilization of such dimers.

For the phenalenyl dimer (**4**), the triplet geometry exhibits two local minima and one global minima (see **Figure 3**). The staggered configuration of **4** is −1.7 kcal/mol lower in energy than the eclipsed conformer. The central C···C distance of both the staggered and eclipsed conformer of **4** are longer than the sum of the van der Waals radii where the central C···C bond of the staggered configuration is shorter than that of the eclipsed configuration by 0.27 Å (see **Figure 4**). The most stable arrangement of **4** is represented by an intermediate structure with a rotational dihedral of 40.9° which, in contrast to the staggered and eclipsed geometries, has a shorter central C···C distance (3.42 Å) and is −0.4 kcal/mol lower in energy than the staggered configuration. These results suggest that the triplet state of **4** is a π-complex.

Though the interatomic distances of **5** and **6**, when going from a singlet to triplet state, increase from values of 3.09 Å and 3.28 Å to values of 3.74 Å and 3.86 Å, we
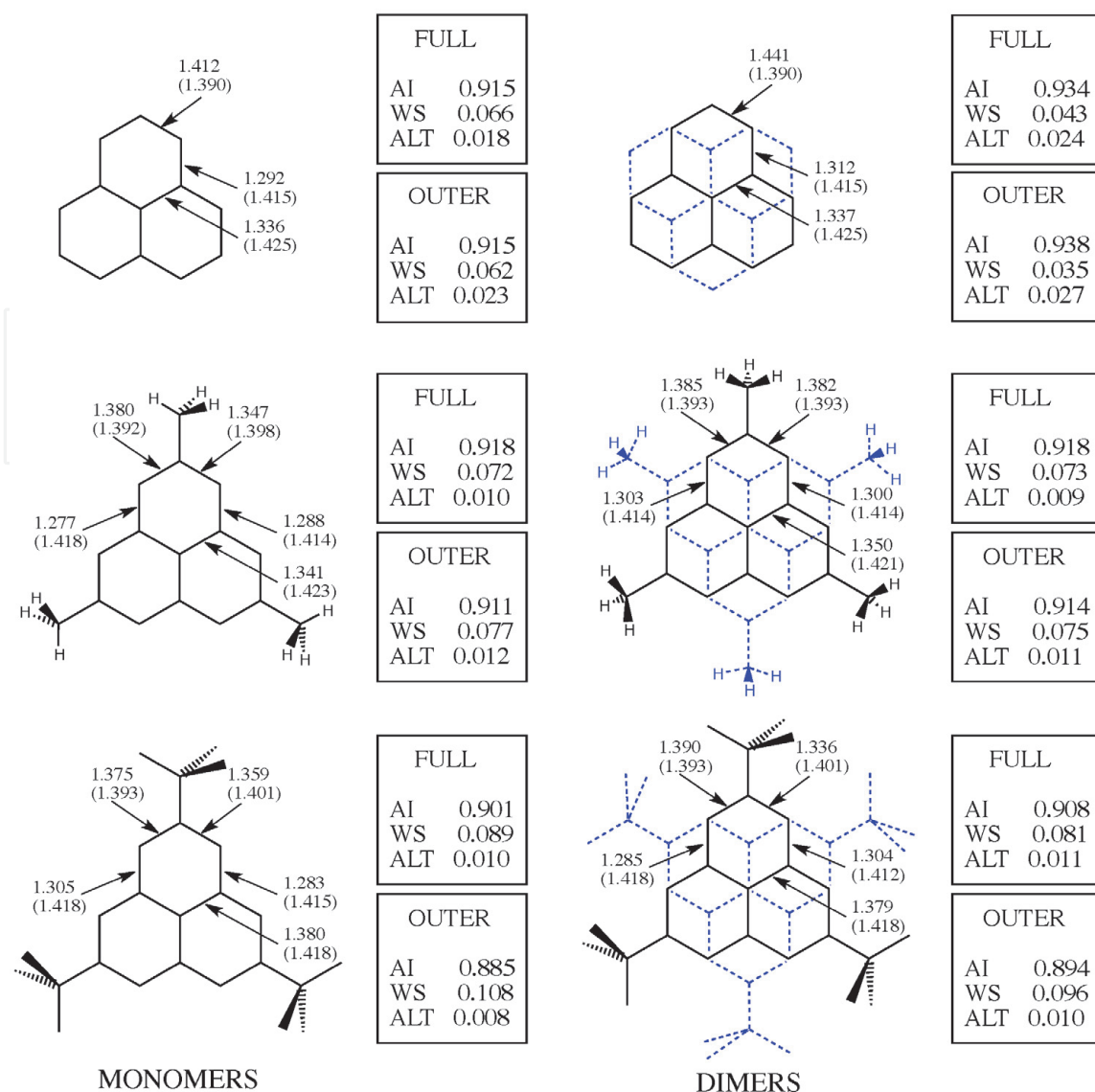
Figure 6.
*Bond strength orders (BSO) and bond lengths (in parentheses, Å) for the phenalenyl, 2,5,8-trimethylphenalenyl and 2,5,8-tri-t-butylphenalenyl radical monomers and dimers (**4** through **6**). The aromaticity delocalization index (AI), bond weakening (strengthening) parameters (WS) and alteration parameters (ALT) for the FULL carbon ring structures (FULL) and the OUTER ring structure (OUTER) are indicated in boxes. The term FULL accounts for all CC bonds while the term OUTER accounts only for outer CC bonds and does not account for the inner most CC bonds.*

observe no change in the rotational alignment between the monomers of the two species. These results suggest that any change in the orientations of **5** and **6** monomers are hindered by their substituent groups. We also note that the ΔE_{ST} values of **4** to **6** steadily decline as substituent size increases (see **Table 2**).

Dissociation energies: From the Morse potential curves of the dichalcodiazoyl dimers **1–3** (C$_2$) bond dissociation energy (BDE$_{calc}$) values of −5.8, −4.7 and −6.0 kcal/mol are obtained, these values being more analogous to the BDE values of electrostatic interactions. The calculated BDE of **1** is in good proximity to the experimental value reported by Beneberu et al. (see **Table 1**). The bond dissociation energy of species **3**, in C$_2$ symmetry, in comparison to **3** in C$_{2v}$ symmetry, is more negative by −2.4 kcal/mol.

The computed bond dissociation energy values for species **4** through **6** are −11.0, −14.8 and −12.4 kcal/mol, respectively. The computed dissociation energy value of **6** is in good agreement with the previously reported experimental enthalpy change (ΔH_D) of −9.5 kcal/mol [59]. We observe the BDE$_{calc}$ of the

2,5,8-trimethylphenalenyl dimer (**5**) to be larger than that of both **4** and **6** by values of 3.8 and 2.4 and kcal/mol suggesting that the addition of three methyl groups to each monomer of the phenalenyl dimer (**5**) yields a more stable dimer as dispersion contributions are enhanced (see **Tables 1** and **2**). In contrast to **5**, the addition of three tert-butyl groups (C4H9) to each monomer of the phenalenyl dimer (**6**) results in a decreased stabilization due to increased steric repulsion between the bulky C4H9 substituents. Moreover, we observe 2,5,8-tri-t-butylphenalenyl dimer (**6**) to be more stable than the phenalenyl dimer (**4**) by 1.4 kcal/mol, indicating that, within **6**, there is a trade-off amongst the steric repulsion of the tert-butyl groups and stabilizing dispersion (see **Table 1** and **Figure 4**).

3.2 Bond parameters and derived bond strength orders n

Di-chalcodiazoyl dimers: As the chalcogen atoms (S, Se, and Te) of the di-chalcodiazoyl dimers (**1**–**3**) increase in atomic radius (see **Figure 5**), the BSO n values of the C···C contacts of **1**–**3** decrease (see **Table 1**). It is noted that C···C contact distances of **1** and **2** are in excellent agreement with experiment (see **Table 1**). The chalcogen···chalcogen contacts within the 1,2,3,5-ditelluradiazolyl dimer (**3**), in C_{2v} symmetry, acquire a k^a value that is smaller than that of the chalcogen···chalcogen interactions of dimers **1** and **2** by 0.147 and 0.109 mdyn/Å, respectively. In the case of the **3**, in C_2 symmetry, N···Te, rather than C···C contacts as observed in **3** (C_{2v}), are seen to coexist alongside Te···Te contacts. Moreover, we find that the BSO n value for the hetero-chalcogen (N···Te) bond of **3** (C_2) is larger than that of the Te···Te contact (see **Table 1**).

In regard to individual aromatic rings of **1**–**3** (i.e. HCNSSN, HCNSeSeN, and HCNTeTeN) we observe the overall bond strength order of each ring (i.e. BSO n (ring)) to decrease as the strength of the chalcogen···chalcogen interactions between corresponding rings decrease in the following order: S···S > Se···Se > Te···Te [BSO n(ring) = 0.214 (**1**), 0.113 (**2**), 0.021 (**3**, C_{2v}), 0.062 (**3**, C_2)]. More-over, as depicted in **Figure 5**, the dimer 1,2,3,5-dithiadiazolyl (**1**) is more stable than the 1,2,3,5-diselenadiazolyl dimer (**2**) by 0.355 mdyn/Å (see **Figure 1**); this result indicates that a greater extent of π-stacking is present within **1** which results in the C···C, N···N, and chalcogen···chalcogen contacts of **1** being shorter than those of **2** (see **Table 1**). Furthermore, the k^a values for the chalcogen···chalcogen contacts (i.e. S···S, Se···Se, and Te···Te) reveal that S···S and Se···Se interactions contribute large amounts of π-delocalization primarily towards the rings, where the overall rings strength of **2** is stronger than that of **3** due to a greater amount of π-delocali-zation from the corresponding chalcogen···chalcogen interactions (Se···Se) (see **Table 1**). From **Figure 5**, in addition to the individual k^a values of the NN, TeTe, NTe, and CC contacts of **3** in C_2 and C_{2v} symmetry, we can see that the C_2 configuration of **3** results in a greater amount of stabilizing π-delocalization, dom-inantly due to the N···N contacts, towards the rings (see **Table 1**). Alongside a decrease in ring strength from **1** to **3** the overall bond length of the aromatic rings, which, in the case of **1** is equivalent to the summation of all R(C-N), R(S-S), and (N-S) bond lengths of a HCNSSN ring, decreases from **1** to **3** (see **Table 1**).

The energy density (H_b) values at the chalcogen···chalcogen (i.e. S···S, Se···Se, and Te···Te) bond critical points r_b of **1**–**3** are negative for **1** and **2** and positive for **3** (see **Table 1**). The negative energy density H_b values at the bond critical points r_b of the chalcogen···chalcogen contacts within **1** and **2** (i.e. S···S, Se···Se) indicate the presence of chalcogen···chalcogen covalent bonding [60]. Positive H_b values of the Te···Te interactions for **3**, in both C_{2v} and C_2 symmetries, indicate that the Te···Te contacts are much weaker than the S···S and Se···Se contacts of **1** and **2** which are of an electrostatic nature. We note that in all cases (**1**–**3**), the H_b values of C···C and

N⋯N contacts are positive. The non-detection of a bond critical point for the C⋯C contacts of **3**, in C_2 symmetry, reveal that such interactions disappear when the C⋯C bond distance stretches slightly beyond that for the equilibrium geometry of **3** (C_{2v}) (see **Table 1**).

From our results we observe that the stabilization of molecules **1** and **2** is primarily due to the large magnitude of π-delocalization from their corresponding chalcogen interactions (i.e. S⋯S and Se⋯Se) where the extent of π-delocalization is seen to correlate in parallel with the strength of the C⋯C contacts and the overall strength of an aromatic rings (see **Table 1**). In contrast to dimers **1** and **2**, **3** (C_{2v}) acquires a much weaker C⋯C contact strengths and an overall weaker aromatic ring strength due to a lesser extent of π-delocalization from the Te⋯Te interactions as revealed from the much smaller k^a (chalcogen⋯chalcogen) values (see **Table 1**). Our results show that the chalcogen bonding does play a stabilizing role in the dimers such as **1** and **2** as suggested by Gleiter and Haberhauer [13, 58, 61], which observe that as pancake bonded species (dimer) are drawn apart the monomers tip outward in such a way that the chalcogen atoms, on each monomer, undergo separation at a slower rate in contrast to their carbon and nitrogen atoms.

Phenalenyl-based dimers: Unlike dimers **1**–**3**, the phenalenyl dimers (**4**–**6**) contain central (interdimer) C–C bonds (see **Figure 1**). As mentioned earlier, in addition to the central C–C bonds of **4**–**6**, we also analyze all peripheral C⋯C bonds which are established between six carbon atoms of each monomer that comprise the corresponding phenalenyl-based dimers (see **Figure 1**). We observe that the central C–C bonds of **4**–**6** decrease in strength from **4** to **6** due to a lesser extent of π-delocalization from peripheral C⋯C as observed from corresponding k^a (C⋯C) values (see **Table 1**). The relative BSO n values of the peripheral C⋯C interactions for all phenalenyl-based dimers (**4**–**6**) are stronger than the corresponding central C–C bonds (see **Table 1**). The k^a values of the central C–C bonds within **4**–**6** are within a range 0.16 and 0.70 mdyn/Å; these bonds are weaker than the C–C single bond in ethane, a classical C–C bond prototype (k^a (C–C) = 4.3 mdyn/Å).

Moreover, the peripheral C⋯C bonds of the phenalenyl dimer (**4**) and of the trimethylphenalenyl dimer (**5**) are shorter than their central C–C bonds (see **Table 1**). For the tri-*tert*-butylphenalenyl dimer (**6**), the interdimer C–C bond is distance is smaller than that of the peripheral C⋯C bonds (see **Table 1**) due to the steric repulsion between the bulky *tert*-butyl groups of the monomers as this repulsion "locks" the dimer into a staggered configuration. The steric repulsion between the *tert*-butyl groups groups of **6** results in a concave pyramidalization of the central CC bonds of the monomers [40], causing the central interatomic C–C bond to be shorter than the outer CC interactions (see **Table 1**). Moreover, the electron density values (ρ_b) of the peripheral C⋯C bonds of **4** and **5** are less than those for the corresponding central C–C bonds and an opposite trend is observed for that **6** (see **Table 1**). We observe both the C⋯C contacts and interdimer C–C interactions of **4**–**6** to have positive energy density values H_b indicating that both interactions acquire an electrostatic nature, rather than a covalent character (see **Table 1**).

3.3 Aromaticity and ring strength of phenalenyl-based monomers and dimers

In order to assess the effect of substitution and dimerization on the monomers and dimers of **4**–**6** we conduct aromaticity delocalization index (AI) analysis. Two AI were determined for each monomer and dimer of **4**–**6**, one AI value considers all CC bonds while the second AI value considers only the outer most CC bonds which trace the species (the inner/central most CC bonds are not considered). In addition to AI values, **Figure 6** lists corresponding WS and ALT parameters, WS gives the weakening/strengthening parameter of the bonds in and *ALT* reflects the

magnitude of bond strength alteration. Overall, the WS and ALT parameters reflect the loss of aromaticity which is attributed to increased structure irregularity. Therefore, the more symmetrical an aromatic perimeter, the greater the aromaticity (i.e. AI) of the system. For example, in the case of benzene, which is planar and very symmetrical as all CC sides (bonds) are identical, the parameters are as follows: WS = 0, ALT = 0, and AI = 1. In general, the smaller the AI the weaker the aromatic character of a species.

Phenalenyl-based monomers: We observe the six outer most CC bonds of the phenalenyl monomer (BSO n(CC) = 1.412) to be identical in strength to those of benzene (BSO n(CC) = 1.451). The addition of methyl substituents to the phenalenyl monomer, in the form of 2,5,8-trimethylphenalenyl, favors a skewed arrangement which places one H atom of every CH_3 group in plane with the phenalenyl rings and the other two H atoms of every CH_3 group above and below the plane of the rings (see **Figure 6**). From the BSO n values and bond distances of the six outermost CC bonds of the 2,5,8-trimethylphenalenyl monomer we observe the outer bonds to be dissimilar (see **Figure 6**). For the CC outer bonds, that are on the same side of the coplaner hydrogen atom of the CH_3 group, CC bond distances and BSO n values increase by 0.002 Å and decrease by 0.032 while that for the CC outer bonds, that are on the same side of the two CH_3 hydrogen atoms above and below the ring, increase by 0.008 Å and decrease by 0.065 in contrast to that of the phenalenyl monomer. A similar trend is observed for the substitution of phenalenyl with t-butyl substituents in the form of 2,5,8-tri-t-butylphenalenyl, where the six outer CC bonds become slightly longer and weaker in contrast to 2,5,8-trimethyl-phenalenyl (see **Figure 6**). In comparison to the phenalenyl monomer the CC outer bonds of 2,5,8-tri-t-butylphenalenyl, which are on the same side of the coplaner methyl group, become longer by 0.003 Å and weaker by 0.037 BSO n units while that for the outer CC bonds, that are on the same side of the methyl groups above and below the ring, stretch by 0.011 Å and decrease in strength by 0.053 units. For the outer CC bonds, not affiliated with the point of substituent attachment (periphery CC bonds), the effect of substitution is too a lesser extent with bond lengths ranging between 1.412 to 1.415 Å and the BSO n(CC) values ranging from 1.283 to 1.312. We note that **6** acquires the weakest outer and periphery CC bonds. Conversely, the three bonds which radiate from the central C (i.e. inner CC bonds) increase in strength from **4** to **5** and from **5** to **6** (see **Figure 6**). This indicates that electron density lost by the deformation of the outer CC bonds, occurring from monomer of **4** to **6**, redistributes to the inner bonds.

The AI (full/outer) values of the phenalenyl monomer are both 0.915. From monomers **4** to **6** we observe the AI, based upon the outer CC bonds, to decrease steadily while the AI, based upon all CC bonds, fluctuates. From the AI outer/full values of the phenalenyl (AI (full, outer) = 0.915), 2,5,8-trimethyl-phenalenyl (AI (full, outer) = 0.918, 0.911) and 2,5,8-tri-t-butylphenalenyl monomers (AI (full, outer) = 0.901, 0.885) we observe that the outer rings have a larger degree of π-delocalization than the full ring. From WS and ALT parameters we can see that the decrease in the aromatic character of the outer CC bonds from monomer **4** (WS, ALT = 0.062, 0.023), to **5** (WS, ALT = 0.077, 0.012), to **6** (WS, ALT = 0.108, 0.008) is predominantly due to bond weakening (as indicated by WS). Overall we observe that as the **4** monomer is substituted with CH_3 (**5**) and *tert*-butyl groups (**6**) the outer aromaticity decreases steadily and is predominately governed by bond weakening effects which are attributed to smaller magnitudes of π-delocalization as additional π-delocalization (i.e. electron density) is pushed away from the points of substitution and adjacent (periphery) CC bonds towards the inner most CC bonds as reflected from the increasing inner CC bond strength from **4** to **6**.

Phenalenyl-based dimers: We note that the trend in BSO n values observed amongst the CC bonds of the monomers discussed in the previous section is similarly observed for the CC bonds of their dimers (**4–6**). It is worth mentioning that the AI (outer/full) values for the dimers are greater than that of their monomer components (see **Figure 6**). The phenalenyl dimer **4**, in contrast to its monomer counterpart, has larger outer, peripheral, and central CC bond strength orders (BSO n(CC)) of 1.441, in very close proximity to that of benzene (1.451). We observe that the the *bigger* aromaticity of dimer **4** is predominately attributed to bond strengthening as revealed from a comparison between the WS parameters of the phenalenyl monomer (WS (full/outer) = 0.066, 0.062) and dimer (**4**) (WS (full/outer) = 0.043, 0.035).

From **Figure 6** it is shown that dimers **5** and **6** favor configurations which position the six methyl or *tert*-butyl groups amongst the dimers in an alternating manner yielding a symmetrical arrangement and in turn a stable species. We note that the methyl groups within the lowest energy rotational isomer of dimer **5** do not have the same orientation as those within its monomer as six hydrogen atoms of the CH_3 groups are rotated inward, towards the center of the molecule (see **Figure 6**). From WS and ALT parameters we see that the dimer of 2,5,8-trimethyl-phenalenyl (**5**) has a greater outer CC aromaticity (AI (outer) = 0.911 (monomer), 0.914 (dimer)) than its monomer due to bond strengthening (WS (full, outer) = 0.077 (monomer), 0.075 (dimer)). We note that this result is consistent with the BSO n values of the peripheral and central CC bonds of dimer **5**, which are greater than those of the monomer by 0.012 to 0.026 units (see **Figure 6**). In contrast to the phenalenyl dimer (**4**), **5** has much larger WS (full/outer) and smaller ALT (full/outer) parameters, where the WS parameters are more altered than the ALT parameters (see **Figure 6**). These results reveal that the aromaticity of the 2,5,8-trimethylphenalenyl dimer (**5**) (AI (full/outer) = 0.918, 0.914) is *less* than that of the phenanlenyl dimer (AI (full/outer) = 0.934, 0.938) primarily due to bond weakening (indicated by WS, see **Figure 6**). The outer/full AI values of the 2,5,8-tri-t-butylphenalenyl dimer (**6**) are both *bigger* than its monomer counterpart being primarily due to bond strengthening as observed from the smaller WS (outer/ full) parameters of the dimer in contrast to that of it monomer (see **Figure 6**). It is also notable that changes in AI (outer/full), when comparing monomer to monomer, monomer to dimer, or dimer to dimer, do not correspond directly to changes in CC bond lengths, in some instances these lengths stay the same or do not drastically change unlike BSO n (CC) orders (see **Figure 6**).

From our results, it is clear that substituents not only prevent σ-dimer formation but reduce the overall aromaticity of both phenalenyl-based monomers and the dimers. As noted, the dimeric systems display a higher AI than the monomeric systems indicating that the dimerization of phenalenyl-based species enhances the aromaticity of the species. Our observation is in line with the nucleus-independent chemical shift (NICS) NMR analysis of Suzuki et al. [21], which suggests that SOMO-SOMO overlap in the dimerized system, overall, supports and stabilizes the aromaticity of the molecules. Furthermore, our work supports the suggestions of Gleiter and Haberhauer who propose that dimers which are pancake bonded undergo stabilization via electron combination as to create a Hückel-allowed [62] (4n + 2 electron) 3-dimensional aromatic system as we observe that, despite the fact that the dimers, unlike their monomers, are not planar (which reduces orbital overlap), the dimers exhibit higher aromaticity. Ultimately, from AI, WS, ALT, and BSO n parameters, we discover that the dimerization of phenalenyl-based monomers increases the aromaticity of the phenalenyl rings predominantly through CC bond strengthening while the substitution of the phenalenyl dimer,

alongside inhibiting σ-dimerization, reduces the overall aromaticity of the system predominantly through CC bond weakening.

4. Conclusions

In this work, we conducted local mode analysis, electron density analysis, and aromaticity delocalization index (AI) calculations (based upon vibrational frequencies) for a set of six neutral pancake-bonded systems, di-chalcodiazoyl dimers (**1–3**) and phenalenyl-based dimers (**4–6**), as to elucidate on the strength of pancake bond interactions within dimers, the ring strength of their monomers, the nature of the pancake bond interactions, the effect of substituents on the aromaticity of phenalenyl-based species, and the effect of dimerization on the aromaticity for phenalenyl-based species. The local stretching force constants, being suitable descriptors of bond strength and π-delocalization, are used to describe the pancake bond interactions of **1–6** and the degree of π-delocalization amongst these bonds and their corresponding dimer species. Directly from computed local stretching force constants we derived bond strength orders. We use measures of AI, and corresponding WS and ALT parameters, to determine what bond property, of the phenalenyl-based species investigated, predominately governs changes in aromaticity. From the results of our work we draw the following: [**1**] We find that dimer species **1** (1,2,3,5-dithiadiazolyl) and **2** (1,2,3,5-diselenadiazolyl) are significantly stabilized by their chalcogen···chalcogen contacts. Unlike **1** and **2**, which have C_{2v} symmtery, the 1,2,3,5-ditelluradiazolyl (**3**) dimer is found to be stable in C_2 symmetry as the singlet state is energetically favored over the triplet state, revealed from a negative ΔE_{ST}. [**2**] In regard to the phenalenyl-based dimers, as the substituent size increased from **4** to **6** the stability of the system steadily declined as the steric repulsion between the substituent groups hindered the monomers of these dimers from changing into a orientation of lower energy. [**3**] As the radius of the chalcogen atoms di-chalcodiazoyl dimers **1–3** increase (Te < Se < S) the strength of the C···C contacts decreases. As the strength of the chalcogen···chalcogen interactions (i.e. contacts) decrease from **1** to **3** the overall ring strength decreases and the strength of the central (i.e. interdimer) C–C bond decreases [**4**]. For all phenalenyl-based dimers (**4–6**) we observed that the BSO n values of peripheral C···C are stronger that of their corresponding central C–C bonds. Revealing that pancake bonding interactions contribute largely to the stability of these species [**5**]. From energy density analysis H_b, following the Cremer-Kraka criteria, we observe the chalcogen···chalcogen pancake bonding interactions of the 1,2-dithia-3,5-diazolyl dimer (**1**) and 1,2-diselena-3,5-diazolyl dimer (**2**) are covalent in nature as they have negative (stabilizing) H_b values at their bond critical point r_b. [**6**] Unlike the other 1,2-chalcogen-3,5-diazole dimers (**1** and **2**) the chalcogen···chalcogen contacts (i.e. Te···Te) of **3** are much weaker in strength and have a positive (destabilizing) energy density value H_b at the Te···Te bond critical point r_b revealing that the Te···Te do not have a typical pancake bond nature as we observed **1** and **2**. [**7**] All pancake bonding interactions within the phenalenyl dimer (**4**), 2,5,8-trimethylphenalenyldimer (**5**), and the 2,5,8-tri-t-butylphenalenyl dimer (**6**) were observed to have postive (destabilizing) H_b values revealing that their pancake interactions are electrostatic in nature. [**8**] From BSO n(CC) values, the calculated AI, and related WS and ALT parameters we found that the dimerization of phenalenyl-based monomers leads to an increased aromaticity primarily due to CC bond strengthening. [**9**] From the same parameters mentioned above we observed that the substitution of the phenalenyl dimer, which is necessary for inhibiting

σ-dimerization, results in an overall reduction of system aromaticity predominantly through CC bond weakening.

Acknowledgements

Author details

Alexis Antoinette Ann Delgado[†], Alan Humason[†] and Elfi Kraka[*]
Southern Methodist University, Dallas, TX, United States

*Address all correspondence to: ekraka@gmail.com

† These authors contributed equally to this work.

IntechOpen

References

[1] Mulliken RS, Person WB. Molecular Complexes: Chapter 16 – Inner and Outer Complexes with π-Acceptors. Hoboken, NJ: Wiley-Interscience; 1969.

[2] Gleiter R, Haberhauer G. Chapter 3: Aromaticity and Other Conjugation Effects. VCH, Weinheim: Wiley; 2012.

[3] Boeré RT. Experimental and computational evidence for "double pancake bonds": The role of dispersion-corrected DFT methods in strongly dimerized 5-aryl-1λ^2,3λ^2-dithia-2,4,6-triazines. ACS Omega. 2018;3(12): 18170–18180.

[4] Kertesz M. Pancake bonding: An unusual pi-stacking interaction. Chem Eur J. 2018;25(2):400–416.

[5] Lemes MA, Mavragani N, Richardson P, Zhang Y, Gabidullin B, Brusso JL, et al. Unprecedented intramolecular pancake bonding in a Dy_2 single-molecule magnet. Inorg. 2020;7(14):2592–2601.

[6] Tonami T, Nagami T, Okada K, Yoshida W, Nakano M. Singlet-fission-induced enhancement of third-order nonlinear optical properties of pentacene dimers. ACS Omega. 2019;4 (14):16181–16190.

[7] Yuan D, Liu W, Zhu X. Design and applications of single-component radical conductors. Chem. 2021 feb;7(2):333–357.

[8] Beneberu H, Tianza Y, Kertesz M. Bonds or not bonds? Pancake bonding in 1,2,3,5-dithiadiazolyl and 1,2,3,5-diselenadiazolyl radical dimers and their derivatives. Phys Chem Chem Phys. 2012;14:10713–10725.

[9] Takano Y, Taniguchi T, Isobe H, Kubo T, Morita Y, Yamamoto K, K Nakasuji, et al. Hybrid density functional theory studies on the magnetic interactions and the weak covalent bonding for the phenalenyl radical dimeric pair. J Amer Chem Soc. 2002;124:11122–11130.

[10] Mouesca JM. Density Functional Theory–Broken Symmetry (DFT–BS) Methodology Applied to Electronic and Magnetic Properties of Bioinorganic Prosthetic Groups. In: Methods in Molecular Biology. Humana Press; 2014. p. 269–296.

[11] Hobza P. The calculation of intermolecular interaction energies. Annu Rep Prog Chem, Sect C: Phys Chem. 2011;107:148.

[12] Mou Z, Uchida K, Kubo T, Kertesz M. Evidence of σ- and π-dimerization in a series of phenalenyls. J Chem Soc. 2014;136:18009–18022.

[13] Gleiter R, Haberhauer G. Electron-rich two-, three- and four-center bonds between chalcogens – New prospects for old molecules. Coord Chem Rev. 2017; 344:263–298.

[14] Mota F, Miller JS, Novoa JJ. Comparative analysis of the multicenter, long bond in [TCNE]$^{.-}$ and phenalenyl radical dimers: A unified description of multicenter, long bonds. J Am Chem Soc. 2009;131:7699–7707.

[15] Takamuku S, Nakano M, Kertesz M. Intramolecular pancake bonding in helical structures. Chem Eur J. 2017;23: 7474–7482.

[16] Nyburg SC, Faerman CH. A revision of van der Waals atomic radii for molecular crystals: N, O, F, S, Cl, Se, Br and I bonded to carbon. Acta Crystallogr B Struct Sci. 1985;41(4):274–279.

[17] Brown JT, Zeller M, Rosokha SV. Effects of structural variations on π-dimer formation: Long-distance multicenter bonding of cation-radicals

of tetrathiafulvalene analogues. Phys Chem Chem Phys. 2020;22(43):25054–25065.

[18] Reid DH. Stable π-electron systems and new aromatic structures. Tetrahedron. 1958;3(3):339–352.

[19] Kubo T. Synthesis, physical properties, and reactivity of stable, π-conjugated, carbon-centered radicals. Molecules. 2019 feb;24(4):665.

[20] Zhong RL, Gao FW, Xu HL, Su ZM. Strong pancake 2e/12c bond in π-stacking phenalenyl derivatives avoiding bond conversion. ChemPhysChem. 2019;20(14):1879–1884.

[21] Suzuki S, Morita Y, Fukui K, Sato K, Shiomi D, Takui T, et al. Aromaticity on the pancake-bonded dimer of neutral phenalenyl radical as studied by MS and NMR spectroscopies and NICS analysis. J Am Chem Soc. 2006;128:2530–2531.

[22] Groom CR, Bruno IJ, Lightfoot MP, Ward SC. The Cambridge structural database. Acta Crystallogr B Struct Sci Cryst Eng Mater. 2016;72(2):171–179.

[23] Small D, Rosokha SV, Kochi JK, Head-Gordon M. Characterizating the dimerizations of phenalenyl radicals by ab initio calculations and spectroscopy: σ-bond formation versus resonance n-stabilization. J Phys Chem A. 2005;109(49):11261–11267.

[24] Andrés J, Ayers PW, Boto RA, Carbó-Dorca R, Chermette H, Cioslowski J, et al. Nine questions on energy decomposition analysis. J Comput Chem. 2019:doi.org/10.1002/jcc.26003.

[25] Kraka E, Zou W, Tao Y. Decoding chemical information from vibrational spectroscopy data: Local vibrational mode theory. WIREs: Comput Mol Sci. 2020;10:1480.

[26] Krapp A, Bickelhaupt FM, Frenking G. Orbital overlap and chemical bonding. Chem Eur J. 2006;12(36):9196–9216.

[27] Zhao L, Hermann M, Schwarz WHE, Frenking G. The Lewis electron-pair bonding model: Modern energy decomposition analysis. Nat Rev Chem. 2019;3(1):48–63.

[28] Cremer D, Pople JA. General definition of ring puckering coordinates. J Am Chem Soc. 1975;97:1354–1358.

[29] Bader RFW. Atoms in Molecules: A Quantum Theory. Oxford: Clarendron Press; 1995.

[30] Wilson EB, Decius JC, Cross PC. Molecular Vibrations. The Theory of Infrared and Raman Vibrational Spectra. New York: McGraw-Hill; 1955.

[31] Kraka E, Larsson JA, Cremer D. Generalization of the badger rule based on the use of adiabatic vibrational modes. In: Grunenberg J, editor. Computational Spectroscopy. New York: Wiley; 2010. p. 105–149.

[32] Delgado AAA, Humason A, Kalescky R, Freindorf M, Kraka E. Exceptionally long covalent CC Bonds – A local vibrational mode study. Molecules. 2021;26:950-1–950-25.

[33] Kalescky R, Kraka E, Cremer D. Description of aromaticity with the help of vibrational spectroscopy: Anthracene and phenanthrene. J Phys Chem A. 2013;118:223–237.

[34] Setiawan D, Kraka E, Cremer D. Quantitative assessment of aromaticity and antiaromaticity utilizing vibrational spectroscopy. J Org Chem. 2016;81:9669–9686.

[35] Krygowski TM, Cyrański MK. Structural aspects of aromaticity. Chemical Reviews. 2001;101(5):1385–1420.

[36] Cremer D, Kraka E. A description of the chemical bond in terms of local properties of electron density and energy. Croatica Chem Acta. 1984;57: 1259–1281.

[37] Kraka E, Cremer D. Chemical implication of local features of the electron density distribution. In: Theoretical Models of Chemical Bonding. The Concept of the Chemical Bond. vol. 2. Z.B. Maksic, ed., Springer Verlag, Heidelberg; 1990. p. 453–542.

[38] Gräfenstein J, Kraka E, Filatov M, Cremer D. Can unrestricted density-functional theory describe open shell singlet biradicals? Int J Mol Sci. 2002;3: 360–394.

[39] Crawford TD, Kraka E, Stanton JF, Cremer D. Problematic p-benzyne: Orbital instabilities, biradical character, and broken symmetry. J Chem Phys. 2001;114:10638–10650.

[40] Cui Zh, Gupta A, Lischka H, Kertesz M. Concave or convex π-dimers: The role of the pancake bond in substituted phenalenyl radical dimers. Phys Chem Chem Phys. 2015;17:23963–23969.

[41] Becke AD. Density-functional exchange-energy approximation with correct asymptotic behavior. Phys Rev A. 1988;38(6):3098–3101.

[42] Lee C, Yang W, Parr RG. Development of the Colle-Salvetti correlation-energy formula into a functional of the electron density. Phys Rev B. 1988;37(2):785.

[43] Chai JD, Head-Gordon M. Long-range corrected hybrid density functionals with damped atom–atom dispersion corrections. Phys Chem Chem Phys. 2008;10(44):6615–6620.

[44] Mardirossian N, Head-Gordon M. Thirty years of density functional theory in computational chemistry: An overview and extensive assessment of 200 density functionals. Mol Phys. 2017; 115(19):2315–2372.

[45] Zhao Y, Truhlar DG. The M06 suite of density functionals for main group thermochemistry, thermochemical kinetics, noncovalent interactions, excited states, and transition elements: Two new functionals and systematic testing of four M06-class functionals and 12 other functionals. Theor Chem Acc. 2008;120(1–3):215–241.

[46] Mou Z, Tian YH, Kertesz M. Validation of density functionals for pancake-bonded π-dimers: Dispersion is not enough. Phys Chem Chem Phys. 2017;19(36):24761–24768.

[47] Zhao Y, Schultz NE, Truhlar DG. Design of density functionals by combining the method of constraint satisfaction with parametrization for thermochemistry, thermochemical kinetics, and noncovalent interactions. J Chem Theory Comput. 2006;2(2):364–382.

[48] Slepetz B, Kertesz M. Volume change during termal [4 + 4] cycloaddition of [2.2](9,10) anthracenophane. J Am Chem Soc. 2013; 135:13720–13727.

[49] Hehre WJ, Ditchfield R, Pople JA. Self—Consistent molecular orbital methods. XII. Further extensions of Gaussian—Type basis sets for use in molecular orbital studies of organic molecules. J Chem Phys. 1972;56(5): 2257–2261.

[50] Clark T, Chandrasekhar J, Spitznagel GW, Schleyer PVR. Efficient diffuse function-augmented basis sets for anion calculations. III. The 3-21+ G basis set for first-row elements, Li–F. J Comput Chem. 1983;4(3):294–301.

[51] Krishnan R, Binkley JS, Seeger R, Pople JA. Self-consistent molecular orbital methods. XX. A basis set for

correlated wave functions. J Chem Phys. 1980;72(1):650–654.

[52] Andrae D, Häußermann U, Dolg M, Stoll H, Preuß H. Energy-adjusted ab initio pseudopotentials for the second and third row transition elements. Theoret Chim Acta. 1990;77: 123–141.

[53] Stoll H, Metz B, Dolg M. Relativistic energy-consistent pseudopotentials-recent developments. Int J Quant Chem. 2002;23:767–778.

[54] Frisch MJ, Trucks GW, Schlegel HB, Scuseria GE, Robb MA, Cheeseman JR, et al. Gaussian 09, Revision C.01. Gaussian, Inc.; 2009.

[55] Zou W, Tao Y, Freindorf M, Makoś MZ, Verma N, Cremer D, et al. Local Vibrational Mode Analysis (LModeA); 2020. Computational and Theoretical Chemistry Group (CATCO), Southern Methodist University: Dallas, TX, USA.

[56] Keith TA. AIMAll (Version 17.01.25). TK Gristmill Software, Overland Park, KS, USA; 2017.

[57] Dimitry Izotov WZ, Cremer D, Kraka E. Ring Puckering Analysis (RING); 2021. Computational and Theoretical Chemistry Group (CATCO), Southern Methodist University: Dallas, TX, USA.

[58] Haberhauer G, Gleiter R. Double pancake versus chalogen-chalogen bonds in six-membered C,N,S-heterocycles. Chem Eur J. 2016;22: 8646–8653.

[59] Small D, Zaitsev V, Jung Y, Rosokha SV, Head-Gordon M, Kochi JK. Intermolecular π-to-π bonding between stacked aromatic dyads. Experimental and theoretical binding energies and near-IR optical transitions for phenalenyl radical/radical versus radical/cation dimerizations. J Am Chem Soc. 2004;126(42):13850–13858.

[60] Oliveira V, Cremer D, Kraka E. The many facets of chalcogen bonding: Described by vibrational spectroscopy. J Phys Chem A. 2017;121:6845–6862.

[61] Gleiter R, Haberhauer G. Long chalogen-chalogen bonds is electron-rich two and four-center bonds: Combination of π- and σ-aromaticity to a three-dimensional σ/π-aromaticity. J Org Chem. 2014;79:7543–7552.

[62] Hückel E. Quantentheoretische Beiträge zum Benzolproblem. I. Die Elektronenkonfiguration des Benzols und Werwandter Verbindungen. Z Phys Chem. 1931;70:204–286.